Biophysical Journal Volume 83 September 2002 1589–1594 1589

Time-Resolved Long-Lived Infrared Emission from Bacteriorhodopsin during its Photocycle

Jianping Wang and Mostafa A. El-Sayed
Laser Dynamics Laboratory, School of Chemistry and Biochemistry, Georgia Institute of Technology, Atlanta, Georgia 30332-0400 USA

ABSTRACT The infrared emission observed below 2000 cm^{-1} upon exciting retinal in bacteriorhodopsin (bR) is found to have a rise time in the submicrosecond time regime and to relax with two exponential components on the submillisecond to millisecond time scale. These time scales, together with the assignment of this emission to hot vibrations from the all-*trans* retinal (in bR) and the 13-*cis* retinal (in the K intermediate), support the recent assignment of the J-intermediate as an electronically excited species (Atkinson et al., *J. Phys. Chem. A.* 104:4130–4139, 2000) rather than a vibrationally hot K intermediate. A discussion of these time scales of the observed infrared emission is given in terms of the competition between radiative and nonradiative relaxation processes of the vibrational states involved.

INTRODUCTION

Bacteriorhodopsin (bR), a protein that is present in the purple membrane (PM) of *Halobacterium salinarium*, functions as a light-driven proton pump (Stoeckenius and Lozier, 1974; Birge, 1981; Mathies et al., 1991; El-Sayed, 1992; Rothschild, 1992; Ebrey, 1993; Lanyi, 1993, 1999; Atkinson et al., 2000). BR has a single polypeptide chain that contains 248 amino acid residues and which is arranged in seven trans-membrane α-helices (Henderson, 1979). The three-dimensional structure of bR has become clear at high resolution by using cryoelectron microscopy (Henderson et al., 1990) and recently by using x-ray crystallography (Pebay-Peyroula et al., 1997; Essen et al., 1998; Luecke et al., 1998, 1999).

The retinal chromophore that is covalently bound to Lys_{216} through a protonated Schiff base (PSB) undergoes the photoisomerization from all-*trans* to 13-*cis* with a quantum efficiency of ~0.6 (Govindjee et al., 1990; Rohr et al., 1992; Logunov et al., 1996), which is much higher than the *trans-cis* photoisomerization efficiency (0.15) of free retinal in methanol (Freedman and Becker, 1986). A cyclic thermal reaction is triggered upon the retinal photoisomerization in bR that involves a series of photointermediates, J, K, L, M_1, M_2, N, and O, with lifetimes ranging from a half picosecond to tens of milliseconds,

$$\begin{aligned} &\text{bR}_{568} \xrightarrow{h\nu} \text{bR}^*_{460} \xrightarrow{500\text{fs}} \text{J}_{625} \xrightarrow{3\text{ps}} \text{K}_{590} \\ &\xrightarrow{1\mu\text{s}} \text{L}_{550} \xrightarrow[-\text{H}^+]{60\mu\text{s}} \text{M}_{1,412} \leftrightarrow \text{M}_{2,412} \\ &\xrightarrow[-\text{H}^+]{\text{ms}} \text{N}_{520} \rightarrow \text{O}_{640} \rightarrow \text{bR}_{568}. \end{aligned}$$

The visible stimulated emission from bR has been well studied (Sharkov et al., 1985; Birge et al., 1987; Mathies et al., 1991; Haran et al., 1996; Ye et al., 1999a,1999b), by using ultrafast optical spectroscopy. A broad stimulated emission band at 640–700 nm (or even to 900 nm), and an intense excited state absorption band at ~460 nm have been found to appear concurrently within 30 fs (Mathies et al., 1991). The rise of the stimulated emission has been demonstrated to be structured, multistaged and wavelength dependent (Ye et al., 1999b). In addition, the decay time of the excited state absorption has been found to be wavelength dependent due to the contribution of the faster decay of stimulated emission. The stimulated emission has a lifetime of 2.5–4 ps, whereas the excited state absorption decay is biexponential (Nuss et al., 1985; Sharkov et al., 1985; Petrich et al., 1987; Mathies et al., 1988; Pollard et al., 1989; Song et al., 1993; Logunov et al., 1996) with a lifetime of 0.5 ps for the large component and of 3–5 ps for the small component.

The photoinduced protein conformational change and retinal configurational change of bR during photocycle have been extensively studied by using low-temperature Fourier transform infrared difference spectroscopy and time-resolved Fourier transform infrared spectroscopy in the mid-infrared (IR) region (Siebert et al., 1982; Maeda et al., 1992; Weidlich and Siebert, 1993; Wolfgang et al., 1996; Dioumaev and Braiman, 1997; Rödig et al., 1999). Very recently, the spectrally resolved IR emission of bR has been reported (Terpugov and Degtyareva, 2001): under steady-state photoexcitation, the majority of the observed emission peaks in the mid-IR region have been attributed to the retinal chromophore in the ground state and in the K intermediate. However, no emission kinetics have been reported. In the present study, we examined the time-resolved emission in the mid-IR region for bR under pulsed visible laser excitation. The observed results are discussed in terms of the change of the retinal configuration and the change of its amino acid environments during the photocycle.

Submitted July 10, 2001 and accepted for publication May 8, 2002.

Dr. Wang's present address is Department of Chemistry, University of Pennsylvania, Philadelphia, PA 19104.

Address reprint requests to Mostafa A. El-Sayed, Laser Dynamics Laboratory, School of Chemistry and Biochemistry, Georgia Institute of Technology, Atlanta, GA 30332-0400. Tel: 404-894-0292; Fax: 404-894-0294; Email: Mostafa.El-Sayed@chemistry.gatech.edu.

0006-3495/02/09/1589/06 $2.00

EXPERIMENTAL

Sample

BR was isolated from the *H. salinarium* strain ET1001 according to a general procedure (Stoeckenius and Lozier, 1974), and suspended in H_2O at pH 7. Samples suspended in D_2O were prepared by 6–7 times of centrifugation in D_2O to replace H_2O without further pH adjustment. Retinal-removed bR, bacterioopsin (bO) was prepared by suspending hydroxylamine at pH 8 under yellow light irradiation, according to a previous paper (Wu et al., 1991). Excess hydroxylamine and bR were separated from bO by a few times centrifugation with deionized water. Concentrated sample suspension was fabricated into a pellet between two CaF_2 windows with maximum optical density of ~1.0 in the visible absorption spectrum for bR and 0.5 in the protein amide bands for bO. The sample temperature was controlled at 25°C by using a water/glycerol bathed thermostat (RTE-100, Neslab Instruments Ltd., Newington, NH) and was probed specifically near the sample by a thermal diode probe (Fisher Scientific, Pittsburgh, PA).

Time-resolved emission measurement

The samples were optically excited at 532 nm by using a nanosecond Nd:YAG pulsed laser (Quantum-Ray DCR-3, Spectra Physics, Mountain View, CA), with pulse width of 10 ns and laser energy of 4–6 mJ/pulse at a repetition rate of 10 Hz. A Mercury-Cadmium-Telluride (MCT) detector (Kolmar Technologies, Conyers, GA) with an effective response time of 20 ns equipped with a Magna-IR 860 Fourier transform infrared spectrometer (Nicolet, Madison, WI) (Wang and El-Sayed, 2001) was used to record the emission from bR. This MCT detector gives a linear response with respect to the incident infrared light intensity. The IR emission was recorded by using the ac-coupled output channel of the MCT detector, in combination with three different germanium-based IR band-pass filters in the ranges of 4000–2000, 3200–600, and 2000–600 cm^{-1}. The emission spectral region was further confined to $>1000\ cm^{-1}$ by using CaF_2 windows on which bR samples were made into pellet. Averaged emission data were recorded directly by using a 500 MHz oscilloscope (Lecroy 9350A, Chestnut Ridge, NY) with selected temporal resolutions of 20 ns, 100 ns, or 10 μs. Transient signals were averaged at least over 500 laser shots to improve the signal-to-noise ratio. Kinetics data were further smoothed and analyzed by using Origin (Microcal Software Inc., Northampton, MA).

RESULTS

Figure 1 shows the formation and relaxation of IR emission from native bR at pH 7. Emission was recorded as an averaged signal in the spectral region of 2000–1000 cm^{-1}. It is found that the observed emission shows an apparent rise time constant of ~22 ns (Fig. 1 *a*), which is comparable to the MCT detector response time. The relaxation of emission can be fitted to a biexponential function with lifetimes and relative amplitudes of 120 μs (79%) and 3 ms (21%), as shown in Fig. 1 *b*. To assign the origin of the observed IR emission, different IR band-pass filters have been used in our measurement. This is illustrated in Fig. 2, in which three emission kinetics curves in the first 170-μs time domain have been shown by using three different IR band-pass filters in the spectral regions of 3200–1000, 2000–1000, and 4000–2000 cm^{-1}, respectively. As can been seen, almost no emission signal was observed in the 4000–2000 cm^{-1} spectral region, and the majority of the IR emission is observed only in the spectral region below 2000 cm^{-1}. Emission intensities in Fig. 2 are shown in arbitrary unit, no normalization was carried out to compensate the difference in the transmittance among these filters (the difference is within 15–20% in their transmitted spectral region). The difference in the emission intensity between the spectral regions of 3200–1000 cm^{-1} (*curve a*) and 2000–1000 cm^{-1} (*curve b*) is solely due to the difference in the transmittance between these two filters (the former has slightly higher transmittance), because there is no signal at >2000

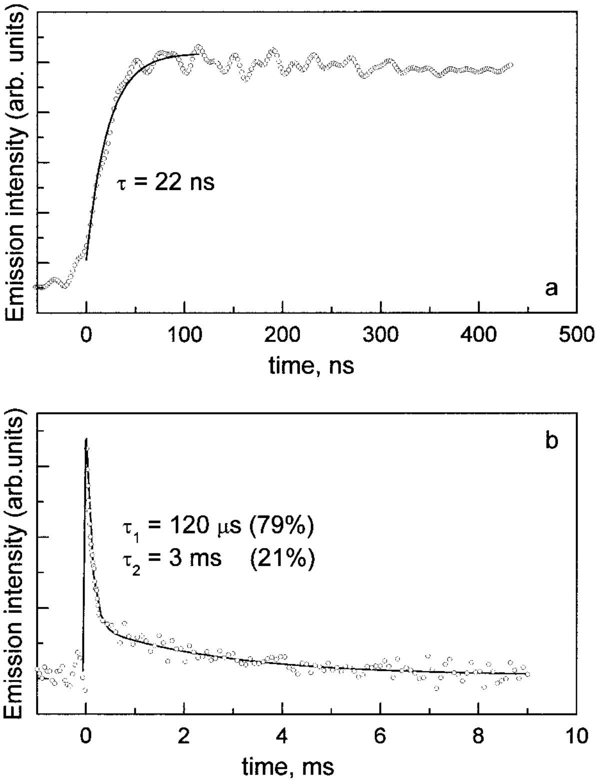

FIGURE 1 IR emission from native bR at pH 7 in the spectral region of 2000–1000 cm^{-1}, after pulsed laser excitation at 532 nm: (*a*) Emission formation within the 450-ns time domain. (*b*) Emission relaxation in the 0–10-ms time domain.

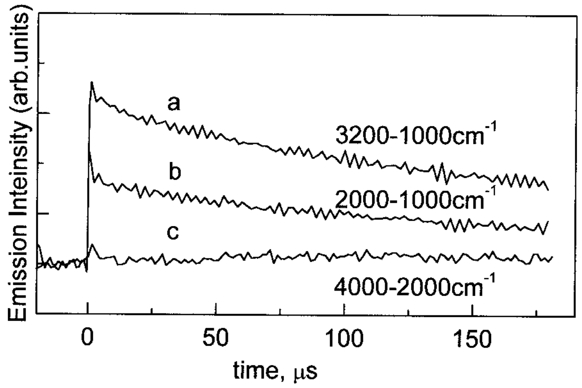

FIGURE 2 Comparison of the IR emission from native bR in H_2O in three different spectral regions: (*a*) 3200–1000 cm^{-1}; (*b*) 2000–1000 cm^{-1} and (*c*) 4000–2000 cm^{-1}. The emission signal difference in the intensity and in the spectral region clearly shows that the IR emission is observed dominantly in the spectral region between 2000 and 1000 cm^{-1} (see text for detail).

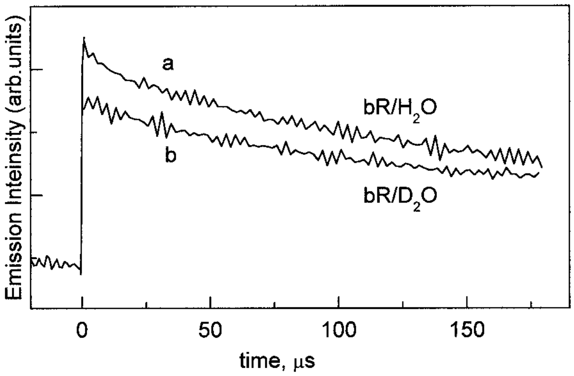

FIGURE 3 A comparison of the IR emission relaxation within the 170-μs time domain: (*a*) native bR in H_2O at pH 7 and (*b*) native bR in D_2O at pH 7. Emission spectra were collected within the spectral region of 3200–1000 cm^{-1} after laser excitation at 532 nm. The result indicates there is no significant difference between the emission signal from H_2O- and D_2O-suspended bR. This suggests that the bR emission is not due to vibrations involving exchangeable hydrogen.

cm^{-1}. In addition, we found that no IR emission from bO was observed at all in the entire mid-IR region, including below 2000 cm^{-1} (data not shown). Because it is known that the photocycle no longer exists and bR loses it bioactivity after the retinal is removed, this result indicates that the observed IR emission signal from bR is associated with the retinal, the protein and its photocycle. No emission observed in bO also excludes the possibility that the emission from bR is related with any black-body radiation that is associated with a few degrees bulk heating of the sample as a result of laser, as one of the reviewers pointed out during the reviewing process of this paper. However, one has to point out that bO does not absorb visible light (532 nm) as well as bR does.

Deuterium effects on the observed bR emission have also been investigated in the present study. Figure 3 shows the emission kinetics within the 170-μs time domain for native bR suspended in H_2O (*curve a*) and D_2O (*curve b*), in the spectral region of 3200–1000 cm^{-1}. The result indicates no significant difference in the emission relaxation between H_2O- and D_2O-suspended bR, which indicates that the observed emission does not result from vibration involving exchangeable hydrogen (e.g., O–H, N–H or H_2O).

The quantum yield of the observed IR emission has been estimated as follows. The incident laser energy I_{las} is 4 mJ/pulse, with a focusing area of 0.5 cm^2 on the sample. The overall resulted IR emission from bR (within the 2000–1000 cm^{-1} spectral range) was evaluated by integrating the response of the MCT detector over time (up to 10 ms), giving the noncalibrated integrated emission response R_{bR}. The response function of the MCT detector was calibrated by modulating the IR beam (static IR beam from a standard commercial globar IR source). The beam has been confined to the 2000–1000 cm^{-1} spectral range by using the same band IR pass filter, with the similar focusing area on the sample as the incident laser. An electronic chopper was used at 100 Hz to create a transient IR pulse on the MCT IR detector, to mimic the integrated transient IR emission (R_{IR}). The calibrated emission intensity from bR (I_{bR}) can be obtained by using

$$I_{bR} = I_{IR} \times \frac{R_{bR}}{R_{IR}}. \tag{1}$$

This is based on the fact that the response of the MCT detector is linear with the incident IR light intensity. Here, I_{IR} is the modulated IR beam intensity (I_{IR} = 0.15 mJ/pulse) to give the emission R_{IR}. Thus the quantum efficiency (Φ) of the observed IR emission from bR is obtained by using

$$\Phi = \frac{I_{bR}}{I_{laser}}. \tag{2}$$

By using Eq. 2, a quantum efficiency of $\Phi \sim 6 \times 10^{-6}$ is estimated as the lower limit for native bR at neutral pH.

DISCUSSION

The recent CW spectroscopic report (Terpugov and Degtyareva, 2001) assigned the emission to originate from retinal in bR (i.e., all-*trans* retinal), from the K-intermediate (13-*cis* retinal), and from some amino acids. It is well established that 40% of the excited all-*trans* bR is de-excited via internal conversion process, i.e., by populating hot vibrational levels of its ground electronic state. The IR emission from bR could then result from the radiative relaxation of some of these 40% of the electronically excited all-*trans* retinal molecules. The other 60% isomerize to the 13-*cis* retinal and to form hot vibrational levels of the 13-*cis* form. This could give an emission signal in the mid-IR region as it relaxes to the K intermediate. In fact, it

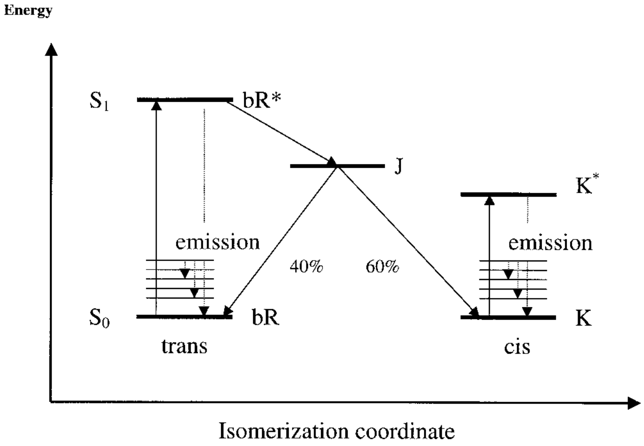

FIGURE 4 The mechanistic diagram of the observed IR emission from bR. A photostationary between all-*trans* and 13-*cis* and their overlap in the visible spectral region allow the formation of K*, the electronically excited K, from which the majority of the IR emission takes place.

was previously thought that J-intermediate has the 13-*cis* form of retinal and is the hot vibrationally excited K (Schulten and Tavan, 1978; Fodor et al., 1988; Dencher et al., 1989; Haupts et al., 1997). If indeed the excited vibrational levels of K formed from the electronically excited all-*trans* retinal are responsible for the observed IR emission, the emission decay time should correspond to the decay of J and the rise of the K-formation (i.e., 3 ps). Because the observed decay of the IR emission is on the micro- to millisecond time scale, the assignment of J being hot vibrational K cannot be correct. This argument supports the recent assignment by Atkinson and coworkers (Ye et al., 1999a; Ujj et al., 2000; Atkinson et al., 2000) that J is in the form of the electronically excited all-*trans* retinal (and not 13-*cis*).

It is known that the electronic excited state of all-*trans* retinal in bR and 13-*cis* in K establish a photostationary mixture in the presence of exciting radiation. The K formed in this manner would absorb the pump laser radiation to form its excited electronic state. Internal conversion from this state could lead to hot vibrational levels of K and thus give the observed IR emission. We believe that this mechanism is dominant in accounting for the origin of the IR emission (Fig. 4). This conclusion is based on the observed lifetime of the emission. If a reasonable amount of the IR emission is due to K formed nonradiatively during the photocycle, the IR emission would have a component with its lifetime corresponding to that of K, which is ~1–2 μs. This lifetime is determined by the rate of the K–L transition. Because the observed IR emission is found to have lifetime longer than 100 μs (120 μs and 3 ms), it cannot be attributed to the K formed during the photocycle. This discussion is based on the assumption that K formed during the photocycle and that formed from the internal conversion of its excited electronic state have quite different vibration populations and thus different modes of vibration relaxation. In other words, we need to distinguish between two types of hot vibration of K. If it comes from bR during the photocycle, it has a lifetime as long as 1 μs but not longer (lifetime of K during the photocycle). However, if this K absorbs a photon to form electronically excited K*, its internal conversion will not necessarily lead to the L photointermediate (in fact some of the K will reisomerize back to the all-*trans* form). Thus its lifetime is not determined by the bR photocycle.

The mechanism we are proposing for the IR emission from K is supported by the observation that the IR emission intensity is sensitive to the exciting wavelength (Terpugov and Degtyareva, 2001). In that study, it is shown that, among many IR emission bands spectrally observed, two bands at 1528 cm^{-1} (due to bR) and 1516 cm^{-1} (due to the K intermediate) can be used to identify the origin of the emission. It was shown that their relative intensities are dependent on the excitation wavelength: 400–750-nm excitation gives higher band intensity at 1528 cm^{-1}, whereas >550-nm excitation only gives higher band intensity at 1516 cm^{-1}. This is more or less in line with the linear absorption spectrum of bR ($\lambda_{\max} \sim 568$ nm) and K ($\lambda_{\max} \sim 590$ nm). We believe that changing the amount of the overlap between the exciting wavelength and the absorption spectrum of K could change the amount of the emission from the K intermediate in two ways. First, it can change the composition of K and bR in the photostationary mixture. Second, it can change the value of the absorption coefficient and thus the amount of radiatively excited K and thus the density of the hot vibrational level in the K-ground electronic state.

The proposed mechanism for K emission suggests that its intensity should depend on the square of the laser power. Unfortunately, to observe the IR emission, pulse energies of the several hundreds μJ are needed. It is possible that, at these power levels, saturation sets in, preventing us from detecting the quadratic dependence.

The IR emission resulting from the amino acids is due to their excited-state vibrational levels. These can be populated either by vibration–vibration energy transfer from the excited retinal modes, or from the retinal isomerization process. During the retinal isomerization process, the protein–retinal configuration suffers a large change. As a result of the Frank–Condon factors in the nonradiative process, it is possible that a number of the bonds of the amino acids that are strongly coupled to the all-*trans* retinal are left vibrationally excited after the retinal isomerization process. It is also possible that the few water molecules near retinal change their configuration and their assembly with the amino acids. This could result in vibrational excitation of not only these water molecules but also their associated amino acids. Because these effects are indirect, the amount of energy converted into their vibration modes is expected to be smaller than that left in the retinal system.

The next question is regarding the observed rise and decay times. The electronic-to-vibrational energy conversion in both electronically excited all-*trans* or 13-*cis* retinal occurs on the pico- to subnanosecond time scale. The observed rise time is the time at which the decaying molecules reach vibrational energy levels where the radiative process (occurs on the ms time scale) begins to compete with the nonradiative processes. The latter can occur as fast as picoseconds and as slow as seconds (e.g., for N_2), depending on the density of the vibrational state and the anharmonicity factors. Both of these parameters decrease as the vibrationally hot molecules relax from higher to lower energy states. Thus, during the cascade processes involved in the relaxation of the vibrational levels of the retinal (and the amino acids), radiative processes become competitive and begin to emit in the mid-IR region. The two decay components on the μs to ms time scale shown in Fig. 1 most likely result from the statistical distributions of the vibrations that have larger anharmonicity factors (which relax on the μs time scale) and those that are more harmonic with high radiative probability and decay on the ms time scale. The large numbers of IR emission peaks observed spectrally (Terpugov and Degtyareva, 2001) could result from transition between excited vibrational levels having different anharmonicity factors and of different vibrational modes of all-*trans* and 13-*cis* retinal (and some of the amino acids). In contrast, it is possible that the short-lived large component is due to emission from the vibrationally excited retinal moiety whereas the weak millisecond component is from emission of excited amino acids (e.g., carbonyl groups).

The authors thank the Chemical Sciences, Geosciences, and Biosciences Division of the Office of Basic Energy Sciences, Office of Sciences, U.S. Department of Energy (under grant DE-FG02–97ER14799) for financial support.

We thank Ms. Christy F. Landes for proof reading the manuscript.

REFERENCES

Atkinson, G. H., L. Ujj, and Y. Zhou. 2000. Vibrational spectrum of the J-625 intermediate in the room temperature bacteriorhodopsin photocycle. *J. Phys. Chem. A.* 104:4130–4139.

Birge, R. R. 1981. Photophysics of light transduction in rhodopsin and bacteriorhodopsin. *Annu. Rev. Biophys. Bioeng.* 10:315–354.

Birge, R. R., L. A. Findsen, and B. M. Pierce. 1987. Molecular dynamics of the primary photochemical event in bacteriorhodopsin. Theoretical evidence for an excited singlet state assignment for the J intermediate. *J. Am. Chem. Soc.* 109:5041–5043.

Dencher, N. A., D. Dresselhaus, G. Zaccai, and G. Bueldt. 1989. Structural changes in bacteriorhodopsin during proton translocation revealed by neutron diffraction. *Proc. Natl. Acad. Sci. U.S.A.* 86:7876–7879.

Dioumaev, A. K., and M. S. Braiman. 1997. Two bathointermediates of the bacteriorhodopsin photocycle, distinguished by nanosecond time-resolved FTIR spectroscopy at room temperature. *J. Phys. Chem. B.* 101:1655–1662.

Ebrey, T. G. 1993. Thermodynamics of membrane receptor channels. *In* Light Energy Transduction in Bacteriorhodopsin. CRC Press, New York. 353–387.

El-Sayed, M. A. 1992. On the molecular mechanisms of the solar to electric energy conversion by the other photosynthetic system in nature, bacteriorhodopsin. *Acc. Chem. Res.* 25:279–86.

Essen, L. O., R. Siegert, W. D. Lehmann, and D. Oesterhelt. 1998. Lipid patches in membrane protein oligomers: crystal structure of the bacteriorhodopsin–lipid complex. *Proc. Natl. Acad. Sci. U.S.A.* 95: 11673–11678.

Fodor, S. P. A., J. B. Ames, R. Gebhard, E. M. M. Van den Berg, W. Stoeckenius, J. Lugtenburg, and R. A. Mathies. 1988. Chromophore structure in bacteriorhodopsin's N intermediate: implications for the proton-pumping mechanism. *Biochemistry.* 27:7097–7101.

Freedman, K. A., and R. S. Becker. 1986. Comparative investigation of the photoisomerization of the protonated and unprotonated n-butylamine Schiff bases of 9-cis-, 11-cis-, 13-cis-, and all-trans-retinals. *J. Am. Chem. Soc.* 108:1245–1251.

Govindjee, R., S. P. Balashov, and T. G. Ebrey. 1990. Quantum efficiency of the photochemical cycle of bacteriorhodopsin. *Biophys. J.* 58: 597–608.

Haran, G., K. Wynne, A. Xie, Q. He, M. Chance, and R. M. Hochstrasser. 1996. Excited state dynamics of bacteriorhodopsin revealed by transient stimulated emission spectra. *Chem. Phys. Lett.* 261:389–395.

Haupts, U., J. Tittor, E. Bambergxda, and D. Oesterhelt. 1997. General concept for ion translocation by halobacterial retinal proteins: the isomerization/switch/transfer model. *Biochemistry.* 36:2–7.

Henderson, R. 1979. The structure of bacteriorhodopsin and its relevance to other membrane proteins. *Soc. Gen. Physiol. Ser.* 33:3–15.

Henderson, R., J. M. Baldwin, T. A. Ceska, F. Zemlin, E. Beckmann, and K. H. Downing. 1990. Model for the structure of bacteriorhodopsin based on high-resolution electron cryo-microscopy. *J. Mol. Biol.* 213: 899–929.

Lanyi, J. K. 1993. Proton translocation mechanism and energetics in the light-driven pump bacteriorhodopsin. *Biochim. Biophys. Acta.* 1183: 241–261.

Lanyi, J. K. 1999. Bacteriorhodopsin. *Int. Rev. Cytol.* 187:161–202.

Logunov, S. L., M. A. El-Sayed, L. Song, and J. K. Lanyi. 1996. Photoisomerization quantum yield and apparent energy content of the K intermediate in the photocycles of bacteriorhodopsin, its mutants D85N, R82Q, and D212N, and deionized blue bacteriorhodopsin. *J. Phys. Chem.* 100:2391–2398.

Luecke, H., H.-T. Richter, and J. K. Lanyi. 1998. Proton transfer pathways in bacteriorhodopsin at 2.3 angstrom resolution. *Science.* 280: 1934–1937.

Luecke, H., B. Schobert, H.-T. Richter, J.-P. Cartailler, and J. K. Lanyi. 1999. Structural changes in bacteriorhodopsin during ion transport at 2 angstrom resolution. *Science.* 286:255–260.

Maeda, A., J. M. Pfefferle, J. Sasaki, Y. Shichida, and T. Yoshizawa. 1992. Low temperature FTIR studies on the photointermediates L, M, and N of bacteriorhodopsin. *Springer Proc. Phys.* 68:68–69.

Mathies, R. A., C. H. B. Cruz, W. T. Pollard, and C. V. Shank. 1988. Direct observation of the femtosecond excited-state *cis-trans* isomerization in bacteriorhodopsin. *Science.* 240:777–779.

Mathies, R. A., S. W. Lin, J. B. Ames, and W. T. Pollard. 1991. From femtoseconds to biology: mechanism of bacteriorhodopsin's light-driven proton pump. *Annu. Rev. Biophys. Biophys. Chem.* 20:491–518.

Nuss, M. C., W. Zinth, W. Kaiser, E. Koelling, and D. Oesterhelt. 1985. Femtosecond spectroscopy of the first events of the photochemical cycle in bacteriorhodopsin. *Chem. Phys. Lett.* 117:1–7.

Pebay-Peyroula, E., G. Rummel, J. P. Rosenbusch, and E. M. Landau. 1997. X-ray structure of bacteriorhodopsin at 2.5 angstroms from microcrystals grown in lipidic cubic phases. *Science.* 277:1676–1681.

Petrich, J. W., J. Breton, J. L. Martin, and A. Antonetti. 1987. Femtosecond absorption spectroscopy of light-adapted and dark-adapted bacteriorhodopsin. *Chem. Phys. Lett.* 137:369–375.

Pollard, W. T., C. H. Cruz, C. V. Shank, and R. A. Mathies. 1989. Direct observation of the excited-state *cis-trans* photoisomerization of bacteriorhodopsin: multilevel line shape theory for femtosecond dynamic hole burning and its application. *J. Chem. Phys.* 90:199–208.

Rödig, C., I. Chizhov, O. Weidlich, and F. Siebert. 1999. Time-resolved step-scan Fourier transform infrared spectroscopy reveals differences between early and late M intermediates of bacteriorhodopsin. *Biophys. J.* 76:2687–2701.

Rohr, M., W. Gaertner, G. Schweitzer, A. R. Holzwarth, and S. E. Braslavsky. 1992. Quantum yields of the photochromic equilibrium between bacteriorhodopsin and its bathointermediate K: femto- and nanosecond optoacoustic spectroscopy. *J. Phys. Chem.* 96:6055–6061.

Rothschild, K. J. 1992. FTIR difference spectroscopy of bacteriorhodopsin: toward a molecular model. *J. Bioenerg. Biomembr.* 24:147–167.

Schulten, K. 1978. An isomerization model for the photocycle of bacteriorhodopsin. *Dev. Halophilic Microorg.* 1:331–334.

Schulten, K., and P. Tavan. 1978. A mechanism for the light-driven proton pump of *H. halobium*. *Nature.* 272:85–86.

Sharkov, A. V., A. V. Pakulev, S. V. Chekalin, and Y. A. Matveets. 1985. Primary events in bacteriorhodopsin probed by subpicosecond spectroscopy. *Biochim. Biophys. Acta.* 808:94–102.

Siebert, F., W. Maentele, and W. Kreutz. 1982. Evidence for the protonation of two internal carboxylic groups during the photocycle of bacteriorhodopsin. Investigation by kinetic infrared spectroscopy. *FEBS Lett.* 141:82–87.

Song, L., M. A. El-Sayed, and J. K. Lanyi. 1993. Protein catalysis of the retinal subpicosecond photoisomerization in the primary process of bacteriorhodopsin photosynthesis. *Science.* 261:891–894.

Stoeckenius, W., and R. H. Lozier. 1974. Light energy conversion in *Halobacterium halobium*. *J. Supramol. Struct.* 2:769–774.

Terpugov, E. L., and O. V. Degtyareva. 2001. Infrared emission from photoexcited bacteriorhodopsin: studies by Fourier transform infrared spectroscopy. *J. Mol. Struct.* 565–566:287–292.

Ujj, L., Y. Zhou, M. Sheves, M. Ottolenghi, S. Ruhman, and G. H. Atkinson. 2000. Vibrational spectrum of a picosecond intermediate in the artificial BR5.12 photoreaction: picosecond time-resolved CARS of T5.12. *J. Am. Chem. Soc.*122:96–106.

Wang, J.-P., and M. A. El-Sayed. 2001. Time-resolved FTIR spectroscopy of the polarizable proton continua and the proton pump mechanism of bacteriorhodopsin. *Biophys. J.* 80:961–971.

Weidlich, O., and F. Siebert. 1993. Time-resolved step-scan FT-IR investigations of the transition from KL to L in the bacteriorhodopsin photocycle: identification of chromophore twists by assigning hydrogen-out-of-plane (HOOP) bending vibrations. *Appl. Spectrosc.* 47: 1394–1400.

Wolfgang, H., K. Munsok, H. Frei, and R. A. Mathies. 1996. Protein dynamics in the bacteriorhodopsin photocycle: a nanosecond step-scan FTIR investigation of the KL to L transition. *J. Phys. Chem.* 100: 16026–16033.

Wu, S., E. S. Awad, and M. A. El-Sayed. 1991. Circular dichroism and photocycle kinetics of partially detergent solubilized and partially retinal regenerated bacteriorhodopsin. *Biophys. J.* 59:70–75.

Ye, T., N. Friedman, Y. Gat, G. H. Atkinson, M. Sheves, M. Ottolenghi, and S. Ruhman. 1999a. On the nature of the primary light-induced events in bacteriorhodopsin: ultrafast spectroscopy of native and C13═C14 locked pigments. *J. Phys. Chem. B.* 103:5122–5130.

Ye, T., E. Gershgoren, N. Friedman, M. Ottolenghi, M. Sheves, and S. Ruhman. 1999b. Resolving the primary dynamics of bacteriorhodopsin, and of a 'C13:C14 locked' analog, in the reactive excited state. *Chem. Phys. Lett.* 314:429–434.